Optical Engineering

SPIEDigitalLibrary.org/oe

# Continuous liquid level monitoring sensor system using fiber Bragg grating

Dipankar Sengupta
Putha Kishore

SPIE

# Continuous liquid level monitoring sensor system using fiber Bragg grating

**Dipankar Sengupta**[a,*] **and Putha Kishore**[b]
[a]University of Padova, Department of Information Engineering, Padova 35131, Italy
[b]National Institute of Technology, Department of Physics, Warangal 506004, India

**Abstract.** The design and packaging of simple, small, and low cost sensor heads, used for continuous liquid level measurement using uniformly thinned (etched) optical fiber Bragg grating (FBG) are proposed. The sensor system consists of only an FBG and a simple detection system. The sensitivity of sensor is found to be 23 pm/cm of water column pressure. A linear optical fiber edge filter is designed and developed for the conversion of Bragg wavelength shift to its equivalent intensity. The result shows that relative power measured by a photo detector is linearly proportional to the liquid level. The obtained sensitivity of the sensor is nearly −15 mV/cm.  [DOI: 10.1117/1.OE.53.1.017102]

Keywords: hydrostatic pressure; chemical etching; liquid level; strain; fiber Bragg grating; edge filter.

Paper 131573P received Oct. 14, 2013; revised manuscript received Nov. 28, 2013; accepted for publication Dec. 9, 2013; published online Jan. 6, 2014.

## 1 Introduction

Several measurement technologies are available to detect liquid levels. They are used under specific circumstances. Up to now, for continuous liquid level measurement the most commonly used methods are resistive, radio frequency capacitance, float type vessel gauge, radar, ultrasonic, laser (reflection type), pressure, and vessel-weighing-type load cells.[1,2] All these methods are electric in nature, so they suffer from intrinsic safety concerns. In any electronic device, there are possibilities of generating of heat and short circuit by its components. So an extra cost must be considered to make these techniques suitable for inflammable atmospheres with no risk.

Optical technologies with optical fiber sensors can give a better solution than the conventional sensors used for measuring the temperature, pressure, strain, salinity, rotation, and flow rate because of their passivity, dielectric nature, and immune to electromagnetic interference.[3] Optical fiber liquid level measurement sensors are intrinsically safe in nature with no risk of explosion even under malfunction operation, because inside the tank and the surroundings there are only inert materials such as optical fibers.

A wide range of fiber optic liquid level sensor systems have been reported and partially commercialized for macro level measurement,[4] such as optical radar technique for level measurement,[5] total internal reflection phenomena in optical fiber,[6,7] and Fabry–Perot interferometric technique.[8,9] But most of the reported sensors sense the change in liquid level through modulated light and their multiplexing is complex.

Fiber optic sensors utilizing fiber Bragg gratings (FBGs) received considerable attention due to its wavelength encoded response, linear output, high sensitivity, large dynamic range, self referencing, inline optical connectivity, and compatibility with fiber optical networks.[10] The change in effective refractive index ($n_{\text{eff}}$) and the grating pitch ($\Lambda$) of the FBG were exploited for sensing various physical parameters, such as temperature, strain, refractive index, etc.

In the literature, many techniques were developed and reported to measure the liquid level using the FBG. High sensitive level sensor was proposed using etched FBG and side polished FBG.[11] A level sensor using the FBG embedded on a cantilever that works on buoyancy force was also developed and reported.[12,13] A majority of the FBG-based level sensors need elaborate mechanical arrangement. The liquid level can also be sensed through hydrostatic pressure, but bare FBG shows poor sensitivity to sense pressure. Many techniques were adopted to enhance the pressure sensitivity of the FBG.[14–18] Attempts were also made to sense liquid level through hydrostatic pressure using the FBG.[19–21]

This article presents the design and packaging of small, simple, and low cost sensor head to measure the liquid level using the principle of hydrostatic pressure. The key element of the sensor head is a uniformly thinned (etched) optical FBG and silicone rubber (SR). The article also depicts the results of a simple low-cost interrogator used in the liquid level sensor system.

## 2 Operating Principle

The FBG is a periodic or a quasi-periodic modulation of refractive index inside the core of a photosensitive optical fiber. When light from a broad band source is propagated through the grating, the wavelength that satisfies the Bragg resonance condition will be reflected.[10] The Bragg condition is

$$\lambda_B = 2n_{\text{eff}}\Lambda, \tag{1}$$

where $\lambda_B$ is the reflected Bragg wavelength of the grating.

The FBG is sensitive to strain and temperature. The relative shift of the Bragg wavelength of an FBG, $(\Delta\lambda_B)/\lambda_B$, to the axial strain $\epsilon_z$ experience by the grating along $z$ direction is given by

*Address all correspondence to: Dipankar Sengupta, E-mail: guuptasengupta@gmail.com

0091-3286/2014/$25.00 

$$\frac{\Delta\lambda_B}{\lambda_B} = (1 - p_e)\epsilon_z, \tag{2}$$

where, $\Delta\lambda_B$ is the shift in Bragg wavelength.

$$p_e = \frac{n_{\text{eff}}^2}{2}[p_{12} - \upsilon(p_{11} + p_{12})], \tag{3}$$

$p_e$ is the photo elastic coefficient. $p_{11} = 0.12$ and $p_{12} = 0.27$ are the photo elastic tensors and $\upsilon = 0.16$ is the Poisson ratio of the fiber core, respectively.[10] Thus, for a given axial micro strain, the shift in Bragg wavelength is

$$\frac{\Delta\lambda_B}{\lambda_B} = 0.78\epsilon_z. \tag{4}$$

When axial force $F$ is applied on the FBG, the produced strain $\epsilon_f$ in the FBG is inversely proportional to its cross sectional area "$a$," described by[22]

$$\epsilon_f = \frac{F}{aE_f}, \tag{5}$$

where $E_f$ is the elasticity coefficient ($7 \times 10^{10}$) of the fiber. Pressure can be sensed using the FBG and to enhance the pressure sensitivity of FBG, an arrangement called sensor head has been made. The schematic of the proposed sensor head is shown in Fig. 1. In this arrangement, one FBG with a cross-sectional area "$a$" less than normal fiber is encapsulated in a metal cylinder filled with SR to act as an elastomer (rubber-like material).

The SR is often one or two part polymers, and may contain fillers to improve properties or reduce cost. The SR is generally nonreactive, stable, and resistant to extreme environments and temperatures from −55°C to +300°C, while still maintaining its useful properties.[23]

When the sensing head is immersed in a liquid, hydrostatic pressure, "$P_r$," is applied to side hole of the sensor head. Accordingly, SR is pressurized in all radial directions corresponding to an axial force acting on the round plate and as a result, the FBG experiences a strain along the length which gives a measure of hydrostatic pressure.

The applied hydrostatic pressure and the strain experienced by the FBG is given by[24]

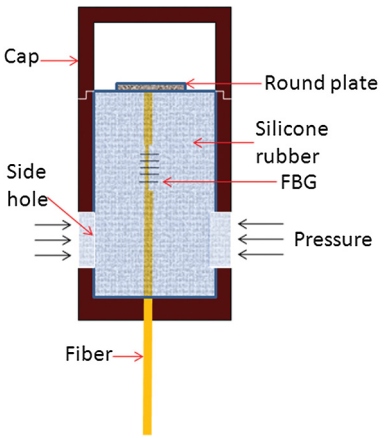


**Fig. 1** Schematic arrangement of hydrostatic pressure sensor head.

$$\epsilon_z = \epsilon_f = \epsilon_{\text{SR}} = \frac{2\nu_{\text{SR}}P_rA}{aE_f + (A - a)E_{\text{SR}}}, \tag{6}$$

where $\epsilon_f$ and $\epsilon_{\text{SR}}$ represent the strains on the fiber and the SR in the designed sensor, respectively. "$A$" is the area of the round plate. $\nu_{\text{SR}}$ and $E_{\text{SR}}$ denote the Poisson's ratio (0.4) and elasticity coefficient ($1.8 \times 10^6$) of the SR, respectively.

Combining Eqs. (2) and (6), the shift in Bragg wavelength of the FBG is

$$\frac{\Delta\lambda_B}{\lambda_B} = (1 - p_e)\frac{2\nu_{\text{SR}}P_rA}{aE_f + (A - a)E_{\text{SR}}}. \tag{7}$$

A vertical column of fluid exerts a pressure due to the column's weight. The relationship between column height and fluid pressure at the bottom of the column is constant for a particular fluid regardless of vessel width or shape. This principle makes it possible to infer the height of liquid in a vessel by measuring the pressure generated at the bottom, i.e., $P = \rho gH$, where "$P$" the hydrostatic pressure, "$\rho$" the density of the liquid, "$g$" acceleration due to gravity, and "$H$" the height of the liquid column.

The relation between water column pressure and hydrostatic pressure is 1 MPa = 102 m. The shift in Bragg wavelength related to water column pressure or water level ($H$) is obtained as

$$\frac{\Delta\lambda_B}{\lambda_B} = (1 - p_e)\frac{204\nu_{\text{SR}}HA}{aE_f + (A - a)E_{\text{SR}}}, \tag{8}$$

where "$H$" represents the water level in meters. Equation (8) shows that the variation in the sensitivity of the sensor for a given water column depends on the physical parameters of the sensor arrangement, i.e., Poisson's ratio and elasticity coefficient of SR, hard core surface area, elasticity coefficient, and cross-sectional area of the fiber, respectively.

## 3 Wet Chemical Etching and Design of Sensor Head

One way to increase the strain sensitivity of the FBG is decreasing the cross-section area of the fiber in which the FBG is written, as given in Eq. (5). This can be done by partially removing the cladding of the fiber, in the region where FBG is written, by a wet chemical etching technique. A range of techniques have been developed for etching optical fibers using concentrated aqueous HF solutions.[25–29] It is important that the FBG-containing fiber has to be uniformly etched because the existence of any surface irregularities can induce corresponding phase perturbations. This leads to perturbations that appear in the form of chirps in the FBG spectrum. Most of the reported techniques have little or no control for ensuring that the etching of the fiber is uniform. For example, dipping technique can produce an etched FBG that can be used in reflection mode only.[25] Iadicicco et al.[29] made another approach, in that the etched FBG can be utilized only within the device employed to etch the fiber. Extra care is required in applying uniform tension during etching when the method involves using epoxy to hold the fiber so that it is immersed in a small well.[27] For example, insufficient tension can lead to a bow-shaped etched fiber with two distinct bent sections that are prone to breakage. In addition to all the above mentioned drawbacks, another practical

limitation often encountered on controlling the length of the fiber to be etched. Hence, a simple etching procedure is required to overcome the practical difficulties in previously reported methods. In the reported work, a novel arrangement of wet chemical etching is illustrated and provides confirmation of the resultant etched fiber.

### 3.1 *Chemical Etching of FBG*

#### 3.1.1 *Fabrication of FBG*

A setup was arranged to write a 3-mm-length FBG. The FBG was fabricated in SM1500(4.2/80) fiber with the standard phase-mask, direct-writing method using a 248-nm Braggstar industrial line narrow excimer laser with pulse energy of 2.56 mJ at 200 Hz. The FBG formation was confirmed by recording its reflection spectrum using an optical spectrum analyzer (OSA) (Ando, AQ 6317B, resolution 10 pm) along with a broad band source and a circulator. A Bragg grating ($\lambda_B = 1550.48$ nm) with 90% reflectivity was formed within 25 s of exposure and is used in the experiment.

#### 3.1.2 *Fiber preparation for etching*

In this reported work, the initial procedure for wet chemical etching of a certain length of an optical fiber that corresponds to the location of FBG was performed in the following steps: (1) find the location and the exact length of the FBG, (2) coat the stripped part of the fiber using Teflon (DuPont, Wilmington, Delaware).

#### 3.1.3 *Wet chemical etching of FBG*

The chemical etching arrangement consists of a "U" shaped clamp made up of Teflon to hold the fiber as schematized in Fig. 2. V–grooves were engraved on the clamp, which was mended for secure and stress free placement of the fiber within the clamp. A Teflon tube of 10-mm-inner diameter was taken. The tube has two 1-mm width slots on the side wall along the diameter of the opening end. The fiber was fixed on the V-grooves of the holder. The movement of the holder was controlled using a one-dimensional translation stage so that the fiber containing FBG can be moved properly through the slot of the Teflon tube. The etching process commenced once the Teflon tube was filled with HF solution. A small volume of silicone oil was added to the HF solution to control the evaporation of HF. This process avoids the usage of a large volume of the HF solution.

It is important to mention that the etching rate depends on the concentration and temperature of the HF solution. Hence, it is necessary to know the rate of etching as diameter of fiber was involved in the experiment. The chemical reaction of HF (40%) solution is exothermic when it reacts with glass.

$$SiO_2 + 4HF \rightarrow SiF_4 + 2H_2O.$$

Prior to chemical etching of FBG, the etching rate was calibrated using the fiber used for the inscription of FBG. Five samples of the fiber were etched for different periods and then immersed in aqueous NaOH solution for deactivating the etching process and further cleaned with deionized water. Photographs of the etched fibers were taken using a microscope.

Using these photographs, the diameter of the etched fibers was determined with the help of MATLAB. Figure 3 shows the plot of fiber diameter against etching time for different temperatures. The graph shows that etching rate depends on surrounding temperature, and it increases with temperature. In addition, etching rate depends on the fiber dopants and their concentration. However, since the fiber samples used in the experiments are of same type, the dependency of chemical etching rate on dopants and their concentration is omitted. The calculation of etching rate is useful so as to know the time required to etch the FBG up to the desired diameter.

The fabricated FBG was chemically etched in 40% HF solution for 10 min at 30°C room temperature using the arrangement shown in Fig. 2. Simultaneously, another fiber of the same type was also chemically etched along with this FBG for the same time period. Using a 10× microscope, photographs of the fiber before and after the etching were taken to record the reduced diameter. The recorded diameter of the fiber and the FBG after the etching was ~4.2/51 $\mu$m. However, no shift in Bragg wavelength of the FBG was observed before or after the chemical etching. No shift in $\lambda_B$ shows that this chemically etched FBG is insensitive to surrounding refractive index perturbation.[26]

### 3.2 *Design of Sensor Head*

The design of the sensor head along with its dimensions is presented in Fig. 4. It consists of a stainless steel hollow cylinder with one side open and a cap for shield this open end. The inner diameter of the hollow cylinder at its opening end is 7.5 mm. A 1-mm hole is drilled at the center of the opposite face of the opening end [Fig. 4(a)]. This is to facilitate

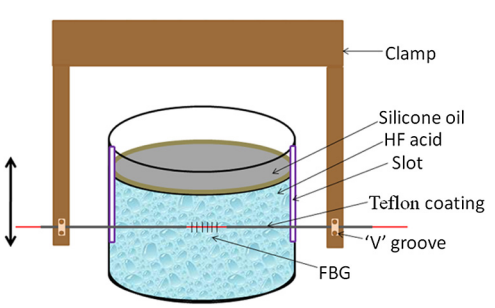


**Fig. 2** Arrangement of wet chemical etching of fiber Bragg grating (FBG).

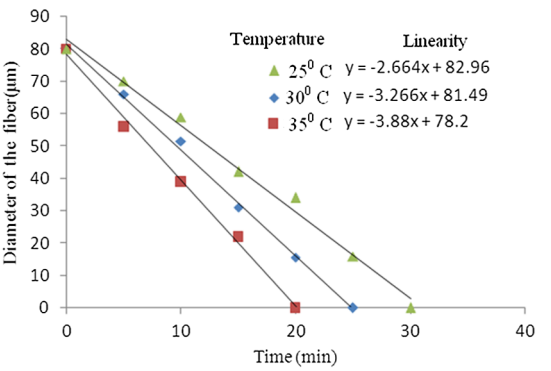


**Fig. 3** Chemical etching rate of the optical fiber at different temperatures.

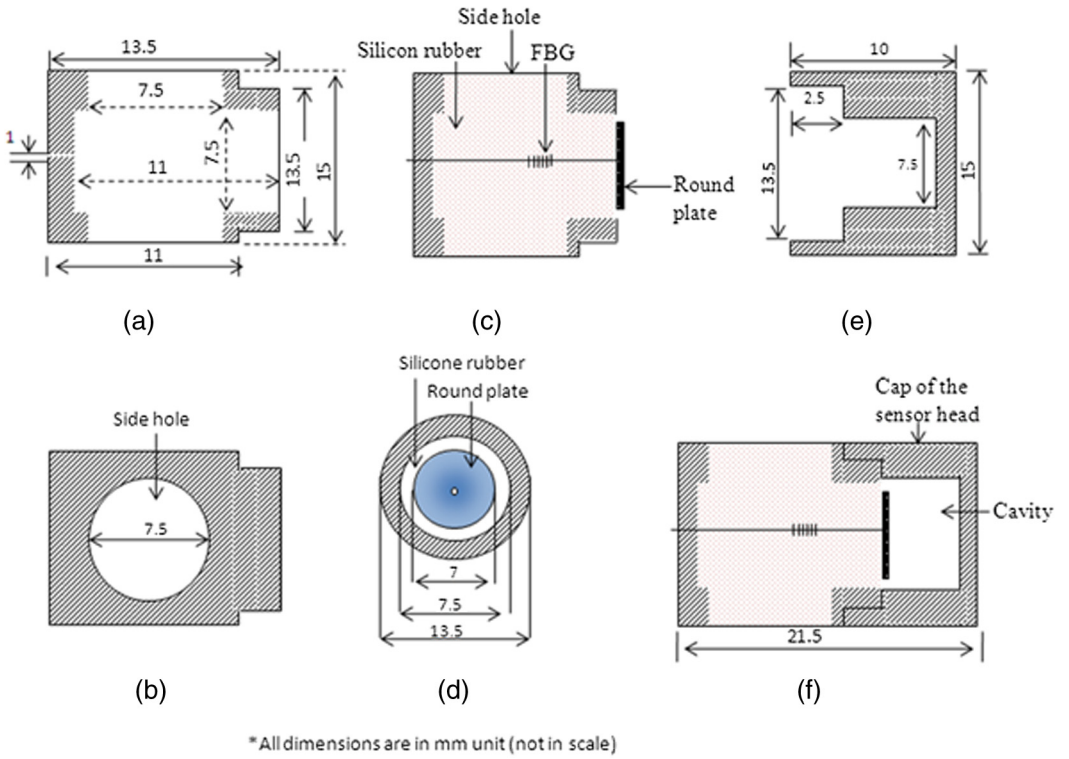


**Fig. 4** Design of the liquid level sensor head.

the optical fiber carrying FBG to pass through the axis of the cylinder. Two side holes with diameters of 7.5 mm on the wall of the hollow cylinder were made normal to the opening end [Fig. 4(b)].

During the preparation of the sensor head, attention was first given to the inserting process of fiber through the 1-mm hole and positioning it to coincide with the axis of the cylinder. Additional care was taken to see that the FBG portion is at the center of the cylinder as shown in Fig. 4(c). Using a 3M tape, the side holes of the hollow cylinder were temporarily sealed. The mixture of SR solution was prepared by mixing homogeneously liquids of SR (KE 1415) and curing agent (CX-32-1417-40) in a ratio of 100:5 by weight. Curing agent is required because SR is a highly-adhesive gel or liquid. Prepared SR solution was poured in the hollow cylinder from its opening end and was kept undisturbed for a time of 48 h at room temperature to get the SR to set. Later, the end of the fiber at the opening end of the cylinder was passed through the 1-mm hole of a round plate (diameter 7 mm) as shown in Figs. 4(c) and 4(d). The tip of the fiber in the center of the round plate was fixed to the round plate using glue. The region of the 1-mm hole through which the fiber passes from the other end was sealed along with the fiber after applying a small axial stress to it. Due to this axial stress, FBG showed a 40-pm shift in Bragg wavelength. This avoids loose shunting of the fiber, and bending and creeping of the FBG in the SR. A cap that fits on the opening end of the cylinder was made up of stainless steel [Fig. 4(e)]. The cap was fixed on the opening end and sealed with glue. Owing to this, an air tight cavity was formed in the cap [Fig. 4(f)]. This air tight cavity allows the SR to elongate toward to the cavity when pressure outside the designed sensor head is greater and induces axial strain in the FBG.

## 4 Experimental Setup and Results

A prototype experimental setup for calculating the liquid level sensitivity of the sensor head is depicted in Fig. 5. The sensor head was installed at the bottom of a liquid container of height 120 cm. The experimental setup consists of a C-band source of 50-nm bandwidth, a circulator, and an OSA (Agilent 86142B).

As the liquid (water) level in the container rises, the hydrostatic pressure at the bottom of the container increases, which results in a shift in the Bragg wavelength of the FBG. The sensor performance was tested within a liquid level range of 0 to 100 cm and with a liquid level increment step of 5 cm.

Figure 6 compares the experimental and theoretical response of the FBG for the rise of the liquid (water) level. The shift in Bragg wavelength of FBG was recorded with an increment of 5 cm. The obtained results show that the

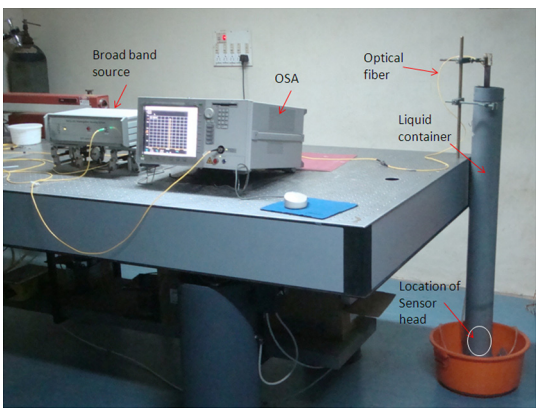


**Fig. 5** Experimental setup for liquid level measurement.

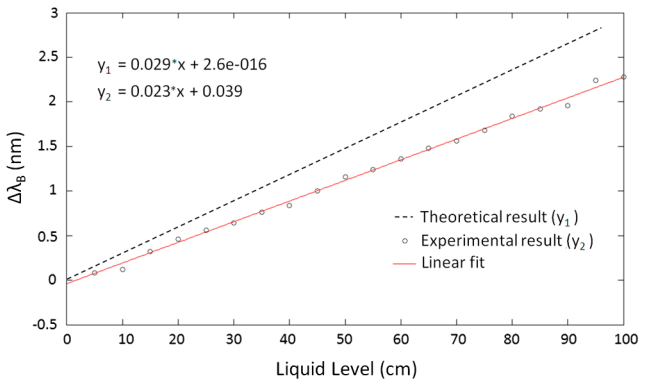


**Fig. 6** Response of the FBG to the rise in liquid level.

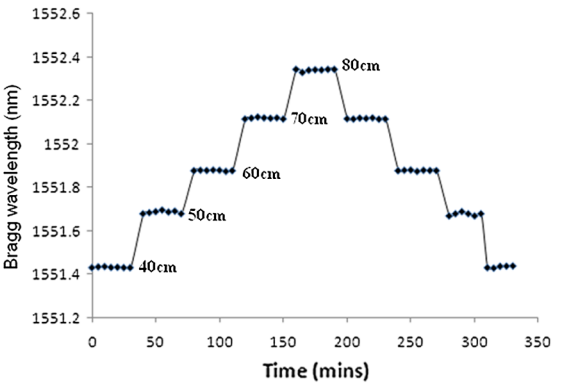


**Fig. 8** Temporal response of the FBG during rise and fall of liquid.

shift in Bragg wavelength was linear with the sensitivity 23 pm/cm. The calculated theoretical sensitivity of the sensor using Eq. (8) is 29 pm/cm, which is slightly higher than the experimental value. The difference in sensitivity between theoretical and experimental results i.e., 6 pm/cm is may be due to the SR stick to the inner wall of the sensor head which leads to decrease in axial force acting on the round plate.

To test the repeatability, the experiment is repeated many times for a liquid column height of 100 cm. The repetition results of the experiment are presented in Fig. 7. A similar spectral shift is found with respect to a change in level.

To study the stability of sensor, a constant liquid level was maintained for a duration of 30 min in steps of 10-cm liquid level variations, and the experimentally obtained sensor response is shown in Fig. 8. The result shows the stability of the sensor at different liquid levels at a tolerance of ±0.01-nm shift in Bragg wavelength. This fluctuation is probably due to vibrations of the liquid in the container. To demonstrate the effect of cross section area of the FBG-containing fiber on liquid level sensitivity, the same experiment was conducted with an FBG written in 9/125-μm photosensitive fiber. The liquid level sensitivity with this FBG is found to be 1.8 pm/cm. The decrease in sensitivity is due to an increase in cross section of the FBG [Eq. (5)]. Thus, in this sensor head arrangement, the liquid level sensing range and sensitivity can be controlled by altering the cross section of the FBG, $E_{SR}$, and "$A$" the radius of the round plate.[15]

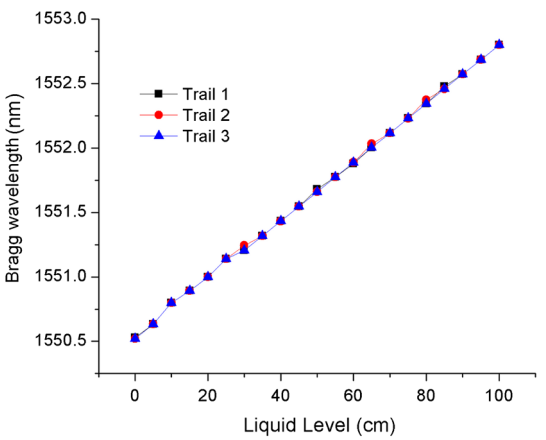


**Fig. 7** Repeatability response of the FBG.

## 5 Detection System

The FBG gives the shift in Bragg wavelength for any change in physical parameters that affect the FBG parameters. In general, OSA is used for measuring the shift in Bragg wavelength. But it is not suitable for real time monitoring applications because of its low scanning frequency, bulkiness, and cost effective. In order to make the detection of change in Bragg wavelength at low cost, a simple intrinsic interference technique is adopted in which single mode-multimode-single mode (SMS) optical fibers are spliced where the diameter of multimode fiber is 100/125 μm. These combinations can be used as edge filters for the selected FBG in use (Fig. 9). The excitation peak wavelength of the SMS is optimized by varying the length of the multimode fiber. When light propagates through one end of the single mode fiber to multimode mode fiber (MMF), this excites a number of guided modes in the MMF.[30] Interference between the different modes occurs when the light propagates through the MMF section. The transmission spectrum of the SMS edge filter for optimized length of 10-cm MMF is shown in Fig. 2. This band-pass response exhibits a two edge-slope response on the either side of a center wavelength of 1553.75 nm. Consequently, this device can be used as an edge filter with either a positive or a negative slope for a selected wavelength range. Here, a negative slope of range 1548 to 1553 nm is considered because the Bragg wavelength of the used FBG is 1550.48 nm.

Figure 10(a) depicts the spectrum obtained from the output of the SMS configuration edge filter. The region between A to B in the figure represents the accepted linear region (negative slope) to convert the shift in Bragg wavelength into its equivalent intensity. Figure 10(b) shows a change in intensity of the reflected Bragg spectrum with the change in liquid levels of 25, 60, and 80 cm, respectively. A low cost photo-detector along with a transimpedance amplifier circuit is used to convert the change in light intensity information

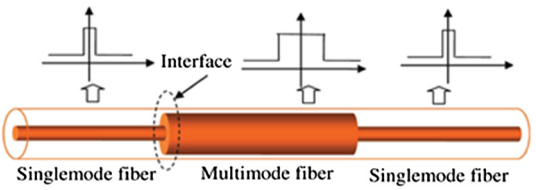


**Fig. 9** The schematic diagram of the SMS configuration.

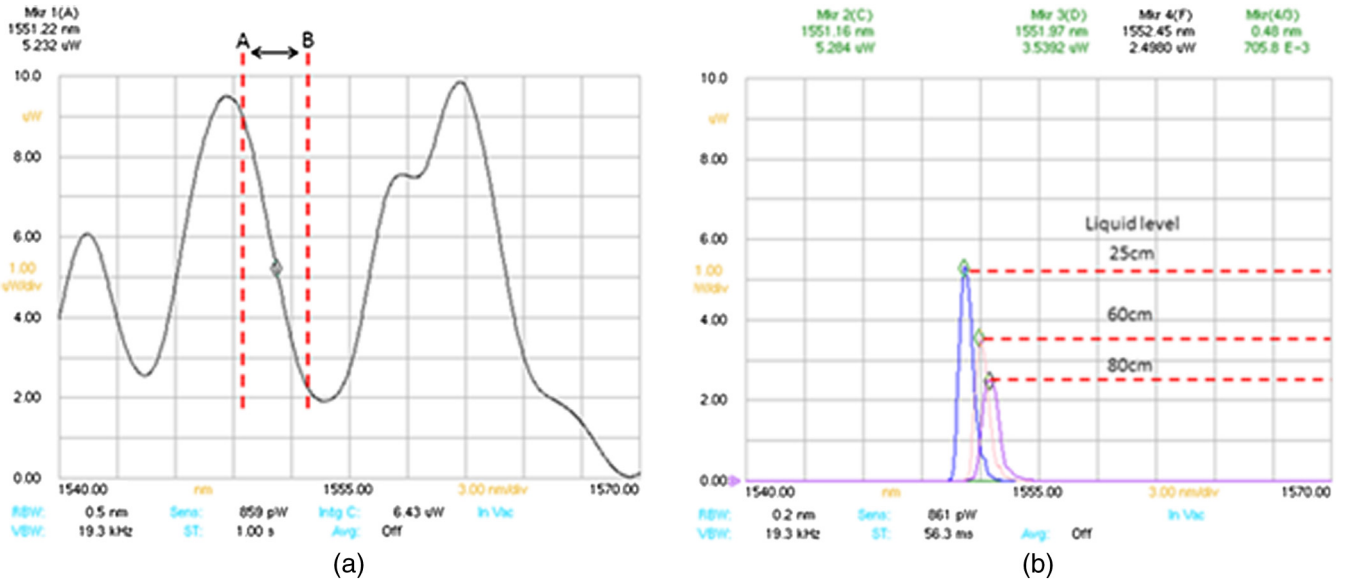


**Fig. 10** (a) Transmission spectrum of the designed SMS edge filter and (b) modulation in the FBG spectrum with change in liquid level.

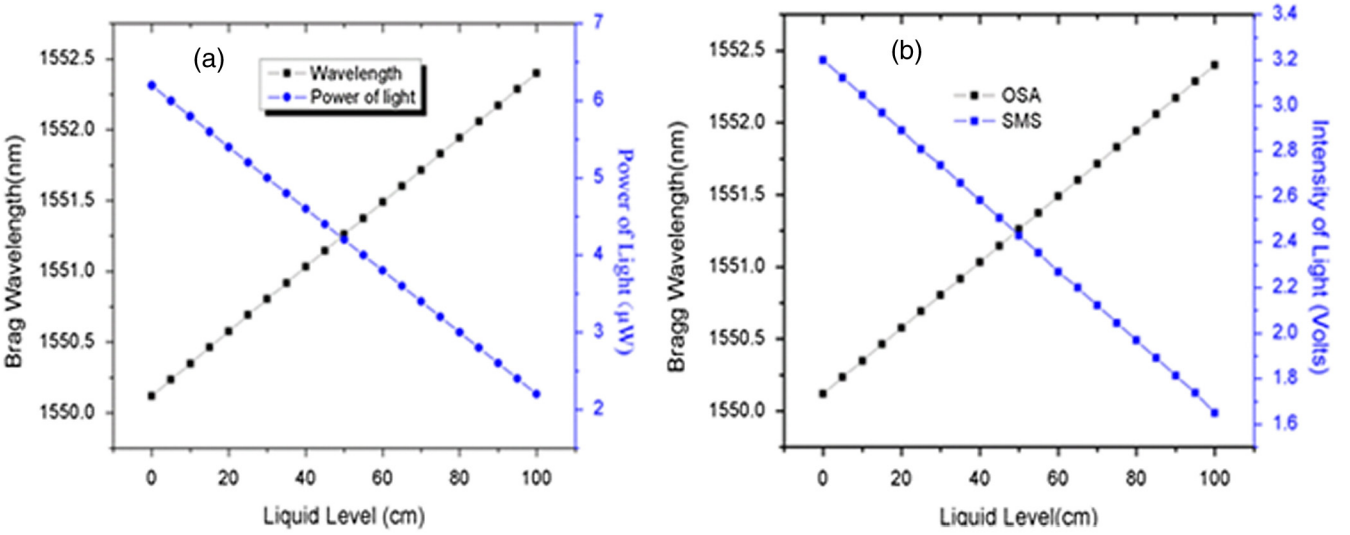


**Fig. 11** The spectral response of the FBG through SMS edge filter.

into a readable voltage signal and is enough to detect the variation of the intensity with respect to the change in liquid level.

Figure 11 shows the output of the shift in Bragg wavelength through the SMS detection system, Fig. 11(a) represents the Bragg wavelength shift as well as power variation with respect to the liquid level measured using the OSA, whereas Fig. 11(b) represents the response of shift in Bragg wavelength detected by the photo-detector. The liquid level sensitivity of the sensor through the detection system is $-15$ mV/cm.

Figure 12 shows the variation of power of reflected Bragg wavelength with respect to the liquid level using both OSA and photo-detector. The above results show that the experimental results of both OSA and the designed detection system of the interrogator are well matched with a linearity of 99%.

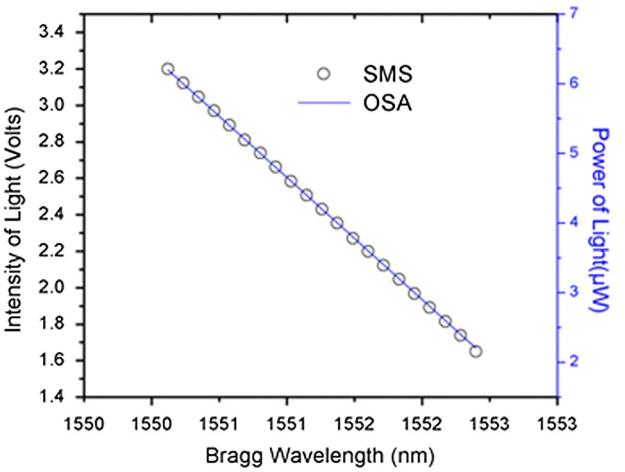


**Fig. 12** The output power variation with resepect to $\lambda_B$.

## 6 Conclusion

In this article, a low cost hydrostatic pressure-based liquid level sensor design and its performance demonstrated. The proposed sensor head length is about 21.5 mm. The sensitivity of the designed sensor head with etched FBG using OSA is found to be 23 pm/cm for a 1-m height of liquid level. The designed sensor head is also compared with another FBG written in 9/125-$\mu$m fiber, and it shows that the sensitivity can be increased with a decrease in cross section area of the FBG, i.e., diameter of the fiber. To achieve an overall low cost of the FBG detection system, an SMS edge filter is incorporated to measure the liquid level. The sensitivity of the detection system is found to be $-15$ mV/cm. This sensor head may find its usage in the industry like at fuel gas station, where liquid kept in a sealed container with low pressure and in open tank, where conventional sensors fail.

### References


1. B. G. Liptak, *Instrument Engineers Handbook: Process Measurement and Analysis*, 3rd ed., Butterworth, Washington, DC (1995).
2. D. R. Gillum, *Industrial Pressure, Level, and Density Measurement*, *ISA Resources for Measurement and Control Series Instrument Society of America*, Research Triangle Park, North Carolina (1995).
3. B. Culshaw and J. Dakin, *Optical Fiber Sensors: Components and Subsystems*, Artech house, Norwood, Massachusetts (1996).
4. D. A. Kron, *Fiber Optical Sensors-Fundamentals and Applications*, Instrument Society of America, North Carolina (1992).
5. K. Iwamoto and I. Kamata, "Liquid-level sensor with optical fibers," *Appl. Opt.* **31**(1), 51–54 (1992).
6. M. Lomera et al., "Lateral polishing of bends in plastic optical fibres applied to a multipoint liquid-level measurement sensor," *Sens. Actuators A* **137**(1), 68–73 (2007).
7. F. Perez-Ocon et al., "Fiber-optic liquid-level continuous gauge," *Sens. Actuators A* **125**(2), 124–132 (2006).
8. Q. Yu and X. Zhou, "Pressure sensor based on the fiber-optic extrinsic Fabry-Perot interferometer," *Photonic Sens.* **1**(1), 72–83 (2011).
9. T. Lü and S. Yang, "Extrinsic Fabry-Perot cavity optical fiber liquid-level sensor," *Appl. Opt.* **46**(18), 3682–3687 (2007).
10. A. Othonos and K. Kalli, *Fiber Bragg Gratings Fundamentals and Applications in Communications and Sensing*, Artech House, London (1999).
11. B. Yun, N. Chen, and Y. Cui, "Highly sensitive liquid-level sensor based on etched fiber Bragg grating," *IEEE Photon. Technol. Lett.* **19**(21), 1747–1749 (2007).
12. T. Guo et al., "Temperature insensitive fiber Bragg grating liquid level sensor based on bending cantilever beam," *IEEE Photon. Technol. Lett.* **17**(11), 2400–2402 (2005).
13. K. R. Sohn and J. H. Shim, "Liquid level monitoring sensor systems using fiber Bragg grating embedded in cantilever," *Sens. Actuators A* **152**(2), 248–251 (2009).
14. Y. Liu et al., "Simultaneous pressure and temperature measurement with polymer-coated fiber Bragg grating," *Electron. Lett.* **36**(6), 564–566 (2000).
15. W. T. Zhang et al., "Ultrathin FBG pressure sensor with enhanced responsivity," *IEEE Photon. Technol. Lett.* **19**(19), 1553–1555 (2007).
16. L. Liu et al., "Membrane based fiber Bragg grating pressure sensor with high sensitivity," *Microw. Opt. Technol. Lett.* **51**(5), 1279–1281 (2009).
17. D. Song et al., "Liquid-level sensor using a fiber Bragg grating and carbon fiber composite diaphragm," *Opt. Eng.* **50**(1), 014401 (2011).
18. H.-S. Huang and T.-C. Liang, "The fabrication and analysis of lateral pressure fiber sensor based on fiber Bragg grating," *Microw. Opt. Technol. Lett.* **50**(10), 2535–2537 (2008).
19. K. Fukuchi et al., "Optical water level sensors using fiber Bragg grating technology," *Hitachi Cable Rev.* **21**(21), 23–28 (2002).
20. P. M. Nellen et al., "Reliability of fiber Bragg grating based sensors for downhole applications," *Sens. Actuator A* **103**(3), 364–376 (2003).
21. D. Sengupta et al., "Sensing of hydrostatic pressure using FBG sensor for liquid level measurement," *Microw. Opt. Technol. Lett.* **54**(7), 1679–1683 (2012).
22. W. Zhou et al., "Simultaneous measurement of force and temperature based on a half corroded FBG," *Microwave Opt. Technol. Lett.* **52**(9), 2020–2023 (2010).
23. Shin-Etsu Silicone, http://www.silicone.jp/e/index.shtml (2013).
24. H.-J. Sheng et al., "A lateral pressure sensor using a fiber Bragg grating," *IEEE Photon. Technol. Lett.* **16**(4), 1146–1148 (2004).
25. A. N. Chryssis et al., "High sensitivity evanescent field fiber Bragg grating sensor," *IEEE Photon. Technol. Lett.* **17**(6), 1253–1255 (2005).
26. A. Iadicicco et al., "Thinned fiber Bragg gratings as high sensitivity refractive index sensor," *IEEE Photon. Technol. Lett.* **16**(4), 1149–1151 (2004).
27. E. R. Lyons and H. P. Lee, "Demonstration of an etched cladding fiber Bragg grating filter with reduced tuning force requirement," *IEEE Photon. Technol. Lett.* **11**(12), 1626–1628 (1999).
28. J. P. Laine, B. E. Little, and H. A. Haus, "Etch-eroded fiber coupler for whispering-gallery-mode excitation in high-Q silica microspheres," *IEEE Photon. Technol. Lett.* **11**(11), 1429–1430 (1999).
29. A. Iadicicco et al., "Refractive index measurements by fiber Bragg grating sensor," in *Proc. IEEE Sensors, 2003*, Toronto, Canada, Vol. 1, pp. 101–105 (2003).
30. Q. Wu et al., "Use of a single-multiple- single-mode fiber filter for interrogating fiber Bragg grating strain sensors with dynamic temperature compensation," *Appl. Opt.* **48**(29), 5451–5458 (2009).



**Dipankar Sengupta** received his MSc degree in physics from Osmania University, India. He received his PhD degree in physics from NIT, Warangal, India, in 2012. Since 2013, he has been working as a postdoctoral fellow in the DEI, University of Padova, Italy. His fields of interest are FOS, FBGs, dynamic Brillouin gratings, and their applications. He is the author and coauthor of 50 international journals and conferences. He is a member of SPIE.

**Putha Kishore** received his MSc degrees from S V University, Tirupati, India in 2008. He is currently pursuing a PhD degree while investigating fiber optics for vibration measurement at the Department of Physics, NIT Warangal, Andhra Pradesh. His research interests include optical fiber vibration sensors, fiber Bragg grating sensors, and specialty fiber optic sensors. He has published 13 articles in journals and 18 articles in conferences. He is a member of SPIE and OSA.